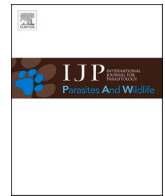


Contents lists available at [ScienceDirect](https://www.sciencedirect.com)

International Journal for Parasitology: Parasites and Wildlife

journal homepage: [www.elsevier.com/locate/ijppaw](http://www.elsevier.com/locate/ijppaw)

## Threatened, host-specific affiliates of a red-listed host: Three new species of *Acanthobothrium* van Beneden, 1849 (Cestoda: Onchoproteocephalidea) from the endangered white skate, *Rostroraja alba* (Lacépède)

Linda Van Der Spuy<sup>a,\*</sup>, Nico J. Smit<sup>a</sup>, Bjoern C. Schaeffner<sup>a,b</sup><sup>a</sup> Water Research Group, Unit for Environmental Sciences and Management, Potchefstroom Campus, North-West University, Hoffman Street, Potchefstroom, 2531, South Africa<sup>b</sup> Institute for Experimental Pathology at Keldur, University of Iceland, Keldnavegur 3, 112 Reykjavík, Iceland

## ARTICLE INFO

## Keywords:

Elasmobranchs  
Affiliate species  
Taxonomy  
Threatened fauna  
Co-extinctions  
Conservation biology  
Marine parasites

## ABSTRACT

The white skate, *Rostroraja alba* (Lacépède), is listed as an endangered species, the second-highest category before being declared extinct in the wild, in the International Union for Conservation of Nature's (IUCN) Red List of Threatened Species. This species is heavily affected by anthropogenic impacts such as capture induced stress by overfishing and by-catch, habitat degradation and pollution that caused a drastic decline in populations in recent years. As part of a larger study on elasmobranch affiliates in southern Africa, two specimens of *R. alba* were screened. Three species of the tapeworm genus *Acanthobothrium* van Beneden, 1849 (Cestoda: Onchoproteocephalidea) were discovered. Application of Ghoshroy and Caira's classification system facilitated the differentiation of congeners through a combination of specific morphological characteristics. As a consequence, three species new to science are described herein, namely *Acanthobothrium umbungus* n. sp., *Acanthobothrium usengozinius* n. sp., and *Acanthobothrium ulondolozus* n. sp. In light of these new discoveries from an endangered host, it is apparent to address the conservation status of its affiliate species, that co-evolved with their elasmobranch hosts for millions of years, thereby creating unique and intimate host-parasite interrelationships. Currently, altering environmental conditions caused by anthropogenic pressures have direct impacts on this host-parasite system with increasing risks of extinction. As merely 9% of elasmobranchs in South African waters have been examined for endohelminths and other affiliate taxa, extensive studies on these organisms and their hosts implementing multisource approaches are needed. This will provide a better understanding on the intimate nature of host-parasite systems that may lead to new prospects in conservation science and the preservation of threatened host species, such as *R. alba*, together with their unique fauna of affiliate species.

## 1. Introduction

Elasmobranchs are currently facing alarming global population declines with 37% of species threatened with a higher risk of extinction, making them the most threatened group of vertebrates in the marine environment (IUCN, 2021). These apex marine predators are heavily affected by anthropogenic impacts, most notably through overfishing and by-catch, and habitat degradation (amongst others) that caused a drastic decline in populations in recent years (Siskey et al., 2019; Sousa et al., 2019). What makes it even more alarming is that elasmobranchs host a variety of affiliate species within and on their bodies, that make up a large proportion of the marine biodiversity (Caira and Healy, 2004;

Zaragoza-Tapia et al., 2020a).

Helminths such as cestodes have co-evolved with their elasmobranch hosts for millions of years (see for instance Dentzien-Dias et al., 2013), thereby creating unique and very intimate host-parasite interrelationships (Caira and Jensen, 2001, 2014). *Acanthobothrium* van Beneden, 1850 (Cestoda: Onchoproteocephalidea II, sensu Caira and Jensen, 2017) is reported to be the most species-rich tapeworm genus known to infect elasmobranchs (Maleki et al., 2015; Caira and Jensen, 2017), currently consisting of 207 valid species (Caira and Jensen, 2017; Zaragoza-Tapia et al., 2019, 2020b; Van Der Spuy et al., 2020). Albeit already being an extremely diverse genus, Caira and Jensen (2017) state that an estimated 800 additional species of *Acanthobothrium* await future

\* Corresponding author. Unit for Environmental Sciences and Management, Potchefstroom Campus, North-West University, Hoffman Street, Potchefstroom, 2531, South Africa.

E-mail address: [Linda.vdspuy@gmail.com](mailto:Linda.vdspuy@gmail.com) (L. Van Der Spuy).

<https://doi.org/10.1016/j.ijppaw.2021.12.010>

Received 14 October 2021; Received in revised form 18 December 2021; Accepted 26 December 2021

Available online 28 December 2021

2213-2244/© 2021 The Authors. Published by Elsevier Ltd on behalf of Australian Society for Parasitology. This is an open access article under the CC BY-NC-ND

license (<http://creativecommons.org/licenses/by-nc-nd/4.0/>).

discovery. Species of *Acanthobothrium* are also known as synhospitalic taxa, exhibiting oioxenous host specificity (Fyler, 2009; Caira and Jensen, 2017). This means that multiple species of *Acanthobothrium* infect a single definitive host species (Caira and Jensen, 2017). This trait could represent a beneficial attribute in providing vital information on the host's biology, life conditions and environmental requirements (Nhi et al., 2013). In recent times, these organisms were also implemented as indicators for ecosystem health assessments (Jankovská et al., 2011; Nhi et al., 2013) and pollution studies (Sures et al., 2017). With increasing threats to elasmobranch host populations and declines in biodiversity, these affiliate species might face even a greater risk of extinction, especially in the cases of highly host-specific taxa such as species of *Acanthobothrium*. Therefore, declines in a single elasmobranch host species will, without a doubt, result in the co-extinction of several affiliate species with potential negative implications for marine ecosystems worldwide (Poulin and Presswell, 2016).

Unfortunately, concurrent with their elasmobranch hosts, research on cestodes and their unique interrelationships with their definitive hosts are ignored and not taken into consideration by conservation agencies. This leaves most of these taxa and their unique ecological services they may provide unknown to science, and render them even more vulnerable to extinction (Poulin and Presswell, 2016; Zaragoza-Tapia et al., 2020a). Acknowledging this research necessity, two specimens of the endangered white skate, *Rostroraja alba* (Lacépède), were screened for cestodes as part of a larger study on elasmobranch affiliates in the understudied ocean basins surrounding southern Africa. By use of light and scanning electron microscopy, we provide taxonomic information on species of *Acanthobothrium*, and describe three species new to science.

## 2. Materials and methods

Specimens for research purposes were obtained with the help of the South African Shark Conservancy (SASC). Ethical approval for this project was received from the North-West University Animal Care, Health and Safety, Research Ethics Committee (NWU-AnimCareREC) with ethics number NWU-00065-19-A5. Permits for the collection and possession of batoid specimens for the purpose of research were issued by the South African Department of Agriculture, Forestry and Fisheries (permit nos. RES2019/58 and RES2019/61 issued to the South African Shark Conservancy).

Two specimens of *Rostroraja alba* [specimen 1: female, mature, 1.85 m in length (tail missing), 1.70 m in disc width, approx. 70 kg in weight, sampling code HE-19-03, fin-clip NB714; specimen 2: female, mature, 2.11 m in length, 1.63 m in disc width, approx. 60 kg, sampling code HE-19-04, fin-clip EC426] were collected by longline in February 2019 from Danger Point, Gansbaai, South Africa [34° 28' 50" S, 19° 19' 55" E]. Both skates were euthanised by use of an adjunctive procedure, inducing neurocranial trauma, pithing the brain immediately thereafter. The spiral intestine, and its contents, of each skate was removed by a mid-ventral incision, and fixed in hot, 4%, neutrally-buffered formalin for morphology and pure ethanol for molecular studies. No specimens were recovered in the ethanol-fixed samples. After a period of two weeks, the spiral intestines and contents were transferred from formalin to 70% ethanol and observed with a stereo microscope. Each individual specimen of *Acanthobothrium* was removed by use of picking tools from both the spiral intestine as well as its contents, and allocated to morphotypes. Specimens of each morphotype were hydrated in a graded ethanol series and stained with Delafield's haematoxylin. Following staining, specimens were again dehydrated in a graded ethanol series to 70%. The overstain of each specimen was cleared in 1% hydrogen chloride. Specimens were then further dehydrated in a grade ethanol series to 100% ethanol, cleared in clove oil, and permanently mounted onto microscope slides in Canada balsam.

Morphological observations were conducted and images of each specimen's various characteristic body structures were acquired by use

of a Nikon Y-TV55 video camera mounted on a Nikon ECLIPSE Ni light microscope (Nikon, Tokyo, Japan). These images were used to obtain measurements for descriptive analyses by use of image analyses software Image Pro Express (Nikon, Japan). Measurements of internal organs, body structures and hooks followed specifications given by

**Table 1**

Metrical information of the three new species of *Acanthobothrium* van Beneden, 1850. Information are presented as the mean, followed by the standard deviation and the number of worms examined. All measurements are in micrometres, unless stated otherwise. Abbreviations: L – length; N – number; W – width.

Character	<i>A. umbungus</i> n. sp.	<i>A. usengozinius</i> n. sp.	<i>A. ulondolozus</i> n. sp.
<b>Total length (mm)</b>	4.23 ± 1.89; 17	7.80 ± 0.92; 7	11.25 ± 1.40; 7
<b>Scolex L</b>	465 ± 30; 17	569 ± 34; 7	561 ± 45; 7
<b>Scolex W</b>	288 ± 49; 17	448 ± 61; 7	409 ± 68; 6
<b>Bothridium W</b>	136 ± 13; 17	233 ± 12; 7	181 ± 10; 6
<b>Anterior (A)</b>	149 ± 15; 14	247 ± 8; 7	205 ± 6; 6
<b>  Ioculus L</b>			
<b>    Middle (M)</b>	84 ± 10; 14	134 ± 6; 7	109 ± 18; 6
<b>    Ioculus L</b>			
<b>  Posterior (P)</b>	78 ± 13; 14	102 ± 5; 7	107 ± 7; 5
<b>  Ioculus L</b>			
<b>Ioculus L ratio (A: M: P)</b>	1.0 : 0.56 ± 0.2 : 0.52 ± 0.3; 14	1.0 : 0.54 ± 0.1 : 0.41 ± 0.1; 7	1.0 : 0.53 ± 0.1 : 0.52 ± 0.1; 5
<b>Muscular pad L</b>	80 ± 9; 14	94 ± 14; 7	136 ± 10; 5
<b>Muscular pad W</b>	106 ± 9; 14	146 ± 10; 7	153 ± 8; 5
<b>Accessory sucker L</b>	24 ± 4; 12	25 ± 2; 7	32 ± 4; 5
<b>Accessory sucker W</b>	38 ± 7; 12	48 ± 5; 7	42 ± 5; 5
<b>Lateral hook A</b>	58 ± 6; 16	68 ± 4; 7	69 ± 6; 6
<b>Lateral hook B</b>	143 ± 9; 16	144 ± 7; 7	157 ± 3; 6
<b>Lateral hook C</b>	115 ± 6; 16	133 ± 5; 7	138 ± 5; 5
<b>Lateral hook D</b>	196 ± 7; 16	203 ± 10; 7	215 ± 3; 6
<b>Medial hook A'</b>	60 ± 5; 17	69 ± 3; 7	68 ± 5; 5
<b>Medial hook B'</b>	143 ± 10; 17	149 ± 10; 7	153 ± 10; 5
<b>Medial hook C'</b>	111 ± 6; 17	132 ± 7; 7	133 ± 9; 5
<b>Medial hook D'</b>	196 ± 11; 17	204 ± 15; 7	207 ± 4; 5
<b>Cephalic peduncle L</b>	457 ± 124; 15	749 ± 211; 7	1244 ± 150; 7
<b>Cephalic peduncle W</b>	82 ± 10; 15	121 ± 2; 7	82 ± 8; 7
<b>Proglottid N</b>	21 ± 4; 17	38 ± 5; 7	40 ± 7; 7
<b>Immature proglottid N</b>	20 ± 4; 17	37 ± 5; 7	37 ± 7; 7
<b>Mature proglottid N</b>	1 ± 1; 17	1 ± 1; 7	3 ± 1; 7
<b>Genital pore position (%)</b>	54 ± 4; 11	51 ± 5; 7	54 ± 4; 7
<b>Terminal proglottid L</b>	907 ± 320; 11	1147 ± 310; 7	1565 ± 389; 7
<b>Terminal proglottid W</b>	273 ± 56; 12	333 ± 39; 7	320 ± 27; 7
<b>Terminal proglottid ratio (L: W)</b>	3 ± 1; 11	3 ± 1; 7	5 ± 1; 7
<b>Cirrus-sac L</b>	138 ± 19; 12	176 ± 33; 6	192 ± 20; 7
<b>Cirrus-sac W</b>	55 ± 12; 12	50 ± 5; 6	66 ± 6; 7
<b>Testis N</b>	33 ± 3; 17	52 ± 8; 6	54 ± 4; 7
<b>Post-poral testis N</b>	5 ± 1; 17	5 ± 1; 7	8 ± 1; 7
<b>Postovarian testis N</b>	0; 17	0; 7	1; 7
<b>Testis L</b>	43 ± 8; 12	54 ± 6; 6	55 ± 5; 7
<b>Testis W</b>	34 ± 3; 12	47 ± 4; 6	44 ± 5; 7
<b>Poral ovarian arm L</b>	386 ± 143; 12	624 ± 56; 6	683 ± 198; 7
<b>Aporal ovarian arm L</b>	434 ± 150; 12	685 ± 58; 6	773 ± 224; 7
<b>Ovary W</b>	95 ± 19; 12	157 ± 14; 6	126 ± 16; 6
<b>Vitelline follicle L</b>	11 ± 3; 17	30 ± 3; 7	17 ± 3; 7
<b>Vitelline follicle W</b>	22 ± 7; 17	19 ± 1; 7	34 ± 8; 7

Ghoshroy and Caira (2001); text descriptions provide the range of measurements only, whereas Table 1 provides additional metrical data including the mean, standard deviation and number of specimens examined. Besides the total length measured in millimetres, all other measurements are presented in micrometres. Line drawings of individual specimens were acquired by use of a drawing attachment tube.

Scanning electron microscopy (SEM) was performed on selected specimens in order to characterise microtrich patterns. Two specimens of each species were cleaned in 70% ethanol from host mucus, and dried by critical point drying. Specimens were then mounted onto carbon tape on aluminium stubs and sputter-coated with carbon (Emscope TB500, Quorum Technologies, Puslinch, Ontario, USA), followed by 20–30 nm gold/palladium (Eiko IB2 ion coater, Eiko, Japan). Each specimen was observed by use of a FEI Nova NanoSEM 450 scanning electron microscope (FEI, Hillsboro, Oregon, USA). Terminology on the microtrich morphology of different scolex regions and strobila follows Chervy (2009). Micrographs were also taken of both immature proglottids (directly posterior to the cephalic peduncle) and mature proglottids (the most anterior region of the terminal proglottid).

Following the most recent species descriptions of *Acanthobothrium*, species determination followed Ghoshroy and Caira's (2001) category classification system to facilitate species characterisations. Species were grouped and assessed based on the following four morphological features: total length of the cestode (<or >15 mm), number of proglottids (<or >50 proglottids), number of testes (<or >80) per proglottid, and the symmetry or asymmetry of aporal and poral ovarian lobes (see Ghoshroy and Caira, 2001). Congeners are distinguished only between members within the same category, as different categories already confirm their dissimilarity in various morphological features (Fyler and Caira, 2006).

All type material has been deposited in the following three helminthological collections: the National Museum, Bloemfontein, South Africa (NMB); the Institute of Parasitology, Biology Centre of the Czech Academy of Sciences, České Budějovice, Czech Republic (IPCAS); and the Natural History Museum, Geneva, Switzerland (MHNG-PLAT). Stubs containing specimens of each species used for SEM were retained in the parasite collection of the Water Research Group, North-West University, South Africa.

### 3. Results

Two, female specimens of the endangered white skate, *R. alba* have been examined for cestode infections. Three, morphologically-distinct species of *Acanthobothrium* were discovered; the first species was found to parasitise the first skate, while the other two species were found in the spiral intestines of the second skate. In addition, few larval stages of a tentaculid species belonging to the order Trypanorhyncha were obtained from the second *R. alba* (data not presented herein).

#### 3.1. *Acanthobothrium umbungus* n. sp. (Figs. 1 and 2)

**Description** (based on whole mounts of 12 mature and five immature worms; two mature worms examined with SEM): Worms 2.4–8.9 mm long, greatest width at level of scolex, 15–32 proglottids per worm, euapolytic. Scolex consisting of scolex proper and cephalic peduncle. Scolex proper with four bothridia, 415–524 long by 225–385 wide. Bothridia free posteriorly, 118–154 wide; each bothridium with three loculi and specialised anterior region in form of muscular pad. Muscular pad 70–96 long by 93–116 wide, falciform in shape, with pronounced posterior margin, bearing accessory sucker and one pair of hooks at posterior margin; accessory sucker 20–30 long by 31–45 wide. Anterior loculus (A) 125–172 long; middle loculus (M) 65–110 long; posterior loculus (P) 60–105 long; loculus length ratio (A: M: P) 1.00 : 0.56: 0.52; maximum width of scolex at level of middle loculus. Velum absent.

Hooks bi-pronged, hollow, with tubercle on proximal surface of axial prongs; internal channels of axial and abaxial prongs continuous,

smooth; axial prongs slightly longer than abaxial prongs; lateral and medial hooks approximately equal in size. Lateral hook measurements: A 49–69, B 127–158, C 102–125, D 183–208. Medial hook measurements: A' 48–71, B' 131–162, C' 101–121, D' 180–216. Bases of lateral and medial hooks approximately equal in length; base of lateral hook slightly overlapping base of medial hook along medial axis of bothridium (Fig. 1D); lateral hook base slightly wider than medial hook base. Tissue covering almost entire length of each prong of hooks. Short cephalic peduncle 291–834 long by 62–97 wide.

Cephalic peduncle densely covered with gladiate spinitriches, filitriches not observed (Fig. 2C). Apical pad and distal bothridial surface covered with acicular filitriches and sparsely interspersed gladiate spinitriches (Fig. 2D). Proximal bothridial surface and bothridial rims covered with gladiate spinitriches, interspersed with acicular filitriches (Fig. 2E). Entire strobila covered in acicular filitriches (Fig. 2F and G).

Proglottids acraspedote. Immature proglottids 16–30 in number; 1–2 mature proglottids; gravid proglottids absent; terminal proglottid 426–1460 long by 165–345 wide; terminal proglottid length to width ratio 2.3–5.4 : 1.0. Proglottids protandrous; genital pores marginal, irregularly alternating (Fig. 1A), 49–65% of proglottid length from posterior margin.

Testes conspicuous in mature proglottids, oval in dorsoventral view, 28–59 long by 27–40 wide, arranged in two to three irregular columns anterior to ovarian isthmus (Fig. 1C), one layer deep, 29–36 in total number, 5–6 in post-poral field. Cirrus-sac pyriform (Fig. 1C), 107–164 long by 35–71 wide, containing armed cirrus; cirrus greatly expanded at base.

Vagina narrow, relatively thin-walled and straight proximally, extending from ootype along medial line of proglottid to anterior margin of cirrus-sac, then laterally at anterior margin of cirrus-sac to common genital atrium. Vaginal sphincter prominent (Fig. 1C). Ovary occupying half of proglottid, almost reaching posterior margin of proglottid, H-shaped in dorsoventral view, lobulated (Fig. 1C), asymmetrical, 60–124 wide at level of ovarian isthmus; poral lobe 139–594 in length; aporal lobe 198–667 in length; ovarian lobes not reaching level of genital opening anteriorly; ovarian isthmus located posterior to mid-level of ovary. Mehlis' gland posterior to ovarian isthmus.

Vitellarium follicular; follicles in two lateral bands, 6–16 long by 10–32 wide, length relative to testis length 0.2–0.4 : 1.0; each band consisting of two columns, extending from posterior margin of anterior-most testes to near posterior margin of ovary (Fig. 1C). Uterus thin-walled, extending from ovarian isthmus to near anterior margin of proglottid (Fig. 1C). Eggs not observed.

Type host: White skate, *Rostroraja alba* (Lacépède) (Rajiformes: Rajidae).

Type locality: Danger Point, Gansbaai, South Africa [34°28'50''S, 19°19'55''E].

Site of infection: Spiral intestine.

Prevalence of infection: 50% (one of two skates examined).

Type material: Holotype deposited at NMB (Accession number: XXX), paratypes in NMB (Accession numbers: XXX-XXX), IPCAS (Accession numbers: XXX-XXX) and MHNG (Accession numbers: XXX-XXX).

ZooBank number for species: XXXXXX.

**Etymology:** The species name “*umbungus*” is derived from “umbungu” [Xhosa; an indigenous language to the Eastern and Western Cape of South Africa] meaning “worm”, referring to the species of tapeworm.

#### Remarks

Following the description of four new species of *Acanthobothrium* by Van Der Spuy et al. (2020), a total of 207 valid species of *Acanthobothrium* are currently recognised worldwide. Ghoshroy and Caira (2001) developed a category classification system that facilitates the differentiation between congeners. *Acanthobothrium umbungus* n. sp. is a

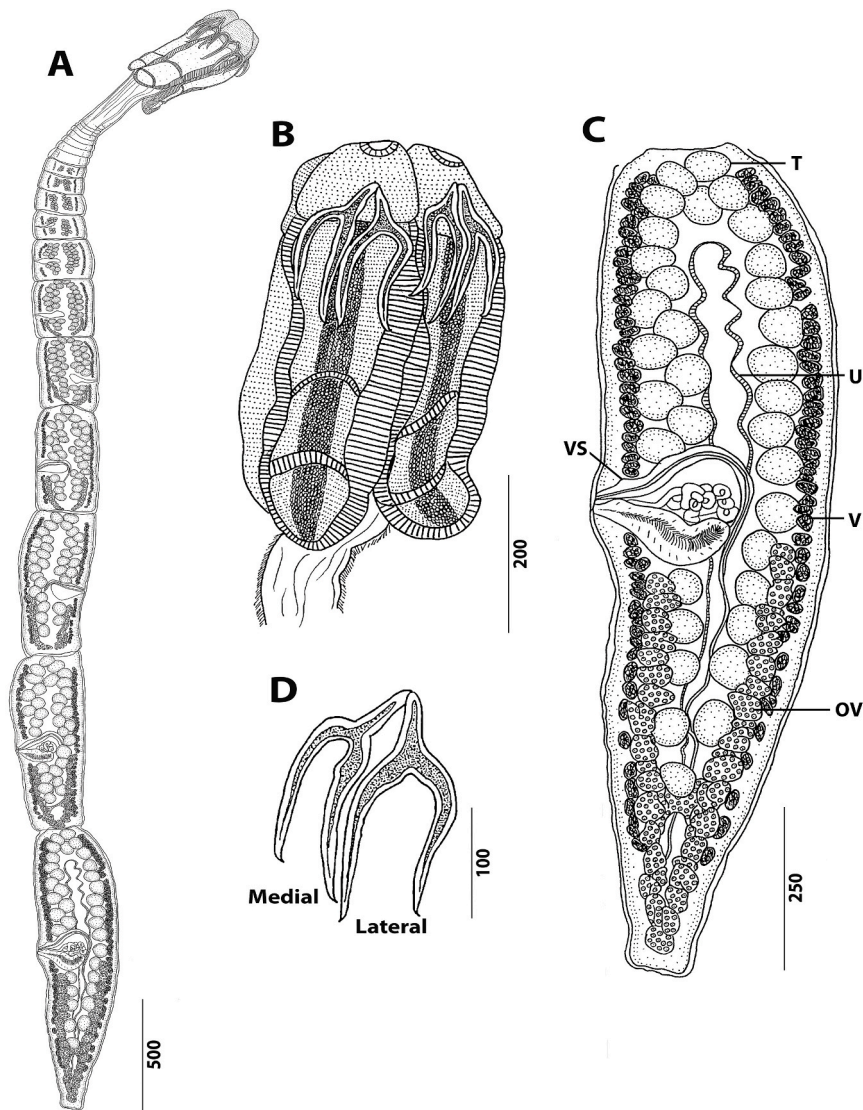


**Fig. 1.** Line drawings of *Acanthobothrium umbungus* n. sp. **A** – entire specimen (holotype; accession no. XXX); **B** – scolex; **C** – mature proglottid (VS, vaginal sphincter; T, testis; U, uterus; V, vitelline follicle; OV, ovary); **D** – hooks.

category 2 species (sensu Ghoshroy and Caira, 2001), with a relatively small body (<15 mm), few segments (<50 in number), few testes (<80 in number) and asymmetrical ovarian lobes. It was therefore compared to 51 congeners with the same category assignment. The most distinguishable feature of *A. umbungus* n. sp. is its hooks, as the hooks of most congeners within this category are much smaller in size (lateral hooks:  $B < 117 \mu\text{m}$  vs  $127\text{--}158 \mu\text{m}$ ,  $C < 102 \mu\text{m}$  vs  $102\text{--}125 \mu\text{m}$ ,  $D < 170 \mu\text{m}$  vs  $183\text{--}208 \mu\text{m}$ ; medial hooks:  $B' < 125 \mu\text{m}$  vs  $131\text{--}162 \mu\text{m}$ ,  $C' < 101 \mu\text{m}$  vs  $101\text{--}121 \mu\text{m}$ ,  $D' < 159 \mu\text{m}$  vs  $180\text{--}216 \mu\text{m}$ , respectively). Based on the hook measurements, *A. umbungus* n. sp. already differs from all but nine species, namely *A. annapienkensis* Carvajal et Goldstein (1971), *A. brayi* Campbell et Beveridge (2002), *A. domingae* Franzese et Ivanov, 2020, *A. gloveri* Campbell et Beveridge (2002), *A. guanghaiense* Yang, Sun, Zhi, Iwaki, Reyda et Yang (2016), *A. popi* Fyler, Caira et Jensen (2009), *A. ppdeleoni* Zaragoza-Tapia, Pulido-Flores et Monks, 2020, *A. tasajerasi* Brooks (1977), and *A. thomasae* Campbell et Beveridge, 2002. The hooks of both *A. annapienkensis* and *A. domingae* exceed that of *A. umbungus* n. sp. (lateral hooks:  $B > 180 \mu\text{m}$  vs  $127\text{--}158 \mu\text{m}$ ,  $C > 125 \mu\text{m}$  vs  $102\text{--}125 \mu\text{m}$ ,  $D > 240 \mu\text{m}$  vs  $183\text{--}208 \mu\text{m}$ , respectively). Besides the differences in hook measurements, *A. brevissime* Linton (1908), *A. campbelli* Marques, Brooks et Monks, 1995, *A. edwardsi* Williams (1969), *A. lasti* Campbell et Beveridge, 2002, *A. minus* Tazerouti et al., 2009, *A. mooreae* Campbell et

Beveridge, 2002, *A. quadripartitum* Williams (1968), *A. sphaera* Maleki, Malek et Palm, 2013, *A. stevensi* Campbell et Beveridge, 2002, *A. thomasae*, *A. tripartitum* Williams (1968), and *A. zapteryicum* Ostrowski de Nunez, 1971, can also be differentiated from *A. umbungus* n. sp. in the following features: a shorter body (<2.4 mm vs 2.4–8.9 mm, respectively), fewer proglottids (<13 vs 15–32, respectively), and fewer testes (<25 vs 29–59, respectively). By comparing the scolex length, *A. brevissime*, *A. campbelli*, *A. chisholmae* Campbell et Beveridge, 2002, *A. dujardini* van Beneden (1850), *A. edwardsi*, *A. hypanus* Zaragoza-Tapia, Pulido-Flores et Monks, 2020, *A. lasti*, *A. lilium* Baer et Euzet, 1962, *A. mashnihae* Fyler et Caira, 2006, *A. microhabentes* Van Der Spuy, Smit et Schaeffner (2020), *A. microtenius* Van Der Spuy, Smit et Schaeffner, 2020, *A. minus*, *A. mooreae*, *A. ppdeleoni*, *A. puntarenasense* Marques, Brooks et Monks, 1995, *A. sinaloansis* Zaragoza-Tapia, Pulido-Flores et Monks, 2020, *A. sphaera*, *A. tasajerasi*, *A. thomasae*, *A. urotrygoni* Brooks et Mayes, 1980, *A. vargasi* Marques, Brooks et Monks, 1995, *A. walkeri* Campbell et Beveridge, 2002, and *A. zapteryicum*, all have a shorter scolex compared to *A. umbungus* n. sp. (<400  $\mu\text{m}$  vs 415–542  $\mu\text{m}$ , respectively). Furthermore, *A. lasti*, *A. microhabentes*, *A. mooreae*, *A. puntarenasense*, *A. rajivi* Ghoshroy et Caira, 2001, *A. sinaloansis*, *A. sphaera*, and *A. urotrygoni* also differ from *A. umbungus* n. sp. in the following features: bothridium width (<112  $\mu\text{m}$

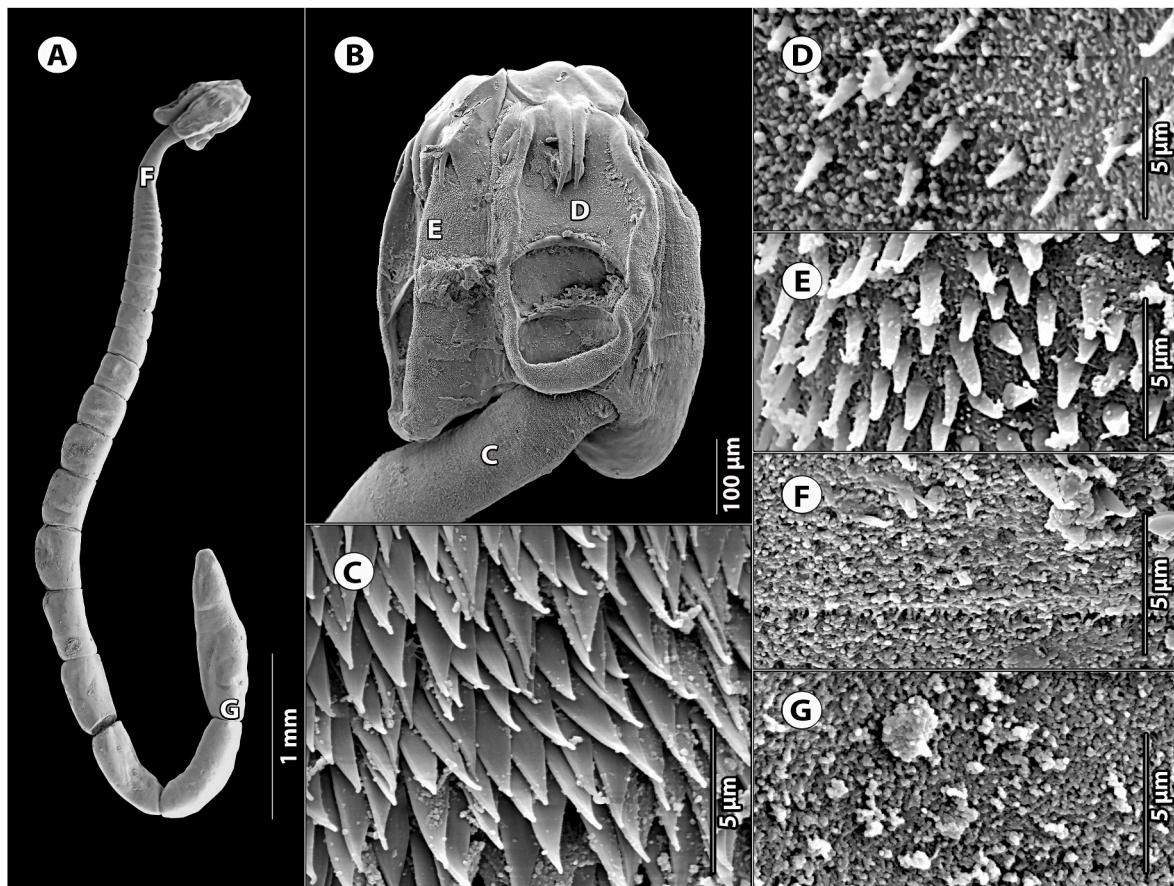


**Fig. 2.** Scanning electron micrographs of *Acanthobothrium umbungus* n. sp. **A** – entire specimen, letters indicate where micrographs of microtriches were taken; **B** – scolex, letters indicate where micrographs of microtriches were taken; **C** – cephalic peduncle; **D** – distal bothridial surface; **E** – proximal bothridial surface, near medial margin of bothridium; **F** – first proglottid; **G** – anterior region of terminal proglottid.

vs 118–154  $\mu\text{m}$ , respectively), middle loculus length ( $<62 \mu\text{m}$  vs 65–110  $\mu\text{m}$ , respectively) and posterior loculus length ( $<56 \mu\text{m}$  vs 60–105  $\mu\text{m}$ , respectively). *Acanthobothrium umbungus* n. sp. can further be distinguished from *A. minus*, *A. mooreae*, *A. sphaera*, *A. tasjerasi*, and *A. thomasa* as they all have a shorter cephalic peduncle ( $<274 \mu\text{m}$  vs 291–834  $\mu\text{m}$ , respectively), whereas *A. chisholmae*, *A. cimari* Marques, Brooks et Monks, 1995, *A. crassus* Van Der Spuy, Smit et Schaeffner, 2020, *A. dolichocollum* Van Der Spuy, Smit et Schaeffner, 2020, and *A. dujardini* all have a longer cephalic peduncle ( $>1000 \mu\text{m}$  vs 291–834  $\mu\text{m}$ , respectively). Furthermore, *A. carolinae* Franzese et Ivanov, 2020, *A. costarricense* Marques, Brooks et Monks, 1995, *A. guanghaiense* and *A. puntarenense* all have a wider cephalic peduncle than that of *A. umbungus* n. sp. ( $>103 \mu\text{m}$  vs 62–97  $\mu\text{m}$ , respectively). Regarding the cirrus-sac and ovary, the length of the cirrus-sac of *A. campbelli*, *A. chisholmae*, *A. mashnihae*, *A. microhabentes*, *A. minus*, *A. soniae* Zaragoza-Tapia, Pulido-Flores, Violante-Gonzalez et Monks, 2019, *A. tetabuanense* Reyda et Caira, 2006, and *A. tripartitum* is  $< 100 \mu\text{m}$  while that of *A. umbungus* n. sp. measures 107–164  $\mu\text{m}$ ; the width of the cirrus-sac of *A. brachyacanthum* Riser (1955), *A. costarricense* and *A. olseni* Dailey et Mudry, 1968 is  $> 84 \mu\text{m}$  versus that of *A. umbungus* n. sp. with 35–71  $\mu\text{m}$ ; and the ovary width of *A. campbelli*, *A. costarricense*, *A. gloveri*, *A. semnovesiculum* Verma (1928), and *A. thomasa* are all  $<53 \mu\text{m}$  while that of *A. umbungus* n. sp. ranges between 60 and 124  $\mu\text{m}$ . *Acanthobothrium umbungus* n. sp. can also be distinguished from *A. bobconniorum* Fyler et Caira, 2010, *A. crassus*, *A. dolichocollum*, *A. microhabentes*, *A. microtenuis*, and *A. popi* by its lack in testes posterior to the ovarian isthmus. Only *A. urotrygoni* and *A. woodsholei* Baer (1948) have a larger body size than *A. umbungus* n. sp. with  $>12 \text{ mm}$  versus 2.4–8.9  $\text{mm}$  (respectively). Additionally, *A. annapienkensis*, *A. brayi*,

*A. bullardi* Ghoshroy et Caira, 2001, *A. domingae* and *A. woodsholei* differ from *A. umbungus* n. sp. in the following features: scolex length ( $>560 \mu\text{m}$  vs 415–542  $\mu\text{m}$ , respectively), bothridium width ( $>176 \mu\text{m}$  vs 118–154  $\mu\text{m}$ , respectively) and cirrus-sac width ( $>85 \mu\text{m}$  vs 35–71  $\mu\text{m}$ , respectively). More species containing a wider bothridium than *A. umbungus* n. sp. are *A. carolinae*, *A. chisholmae*, and *A. costarricense* ( $>161 \mu\text{m}$  vs 118–154  $\mu\text{m}$ , respectively). *Acanthobothrium bobconniorum*, *A. cimari*, *A. costarricense*, *A. crassus*, *A. dujardini*, *A. hypanus*, *A. popi*, *A. puntarenense* and *A. semnovesiculum* all have more testes than *A. umbungus* n. sp. ( $>36$  vs 29–36, respectively).

*Acanthobothrium umbungus* n. sp. represents the third species of *Acanthobothrium* and the seventh cestode record from this host. In southern Africa, only four species of *Acanthobothrium* are currently known (Van Der Spuy et al., 2020). Including *A. umbungus* n. sp., it not only increases the number of species of this genus in the Eastern South Atlantic Ocean but also marks southern Africa as an understudied biogeographical region with the potential of an immense hidden parasite diversity.

### 3.2. *Acanthobothrium usengozinius* n. sp. (Figs. 3 and 4)

**Description** (based on whole mounts of five mature and two immature worms; two mature worms examined with SEM): Worms 6.3–8.8  $\text{mm}$  long, greatest width at level of scolex, 32–45 proglottids per worm, euapolytic. Scolex consisting of scolex proper and cephalic peduncle. Scolex proper with four bothridia, 540–631 long by 372–508 wide. Bothridia free posteriorly, 215–245 wide; each bothridium with three loculi and specialised anterior region in form of muscular pad. Muscular pad 78–109 long by 139–163 wide, falciform in shape, with

pronounced posterior margin, bearing accessory sucker and one pair of hooks at posterior margin; accessory sucker 23–26 long by 43–54 wide. Anterior loculus (A) 235–257 long; middle loculus (M) 126–143 long; posterior loculus (P) 94–106 long; loculus length ratio (A: M: P) 1.00 : 0.54 : 0.41; maximum width of scolex at level of middle loculus. Velum absent.

Hooks bi-pronged, hollow, with tubercle on proximal surface of axial prongs; internal channels of axial and abaxial prongs continuous, smooth; axial prongs slightly longer than abaxial prongs; lateral and medial hooks approximately equal in size. Lateral hook measurements: A 62–73, B 135–151, C 129–141, D 190–216. Medial hook measurements: A' 64–74, B' 139–162, C' 125–142, D' 193–228. Bases of lateral and medial hooks approximately equal in length; base of lateral hook slightly overlapping base of medial hook along medial axis of bothridium (Fig. 3D); medial hook base slightly wider than lateral hook base. Tissue covering almost entire length of each prong of hooks. Short cephalic peduncle 572–1080 long by 119–124 wide.

Cephalic peduncle densely covered with gladiate spinitriches, filitriches not observed (Fig. 4D). Apical pad and distal bothridial surface covered with acicular filitriches and very sparsely interspersed gladiate

spintriches (Fig. 4E). Proximal bothridial surface and bothridial rims covered with gladiate spinitriches, interspersed with acicular filitriches (Fig. 4F). Anterior region of strobila covered in acicular filitriches (Fig. 4G). Anterior region of terminal proglottid covered in capilliform filitriches (Fig. 4H).

Proglottids acraspedote. Immature proglottids 29–44 in number; 1–3 mature proglottids; gravid proglottids absent; terminal proglottid 795–1538 long by 275–394 wide; terminal proglottid length to width ratio 2.5–4.6 : 1.0. Proglottids protandrous; genital pores marginal, irregularly alternating (Fig. 3A), 42–58% of proglottid length from posterior margin.

Testes conspicuous in mature proglottids, oval in dorsoventral view, 42–63 long by 42–51 wide, arranged in one to two layers in inter-vascular field (Fig. 3C), 42–61 in total number, 0 in post-poral field of mature proglottids, 4–5 in post-poral field of immature proglottids. Cirrus-sac obpyriform (Fig. 3C), 151–234 long by 43–57 wide, containing armed cirrus; cirrus greatly expanded at base.

Vagina narrow, relatively thin-walled and straight proximally, extending from ootype along medial line of proglottid to anterior margin of cirrus-sac, then laterally to common genital atrium. Vaginal sphincter

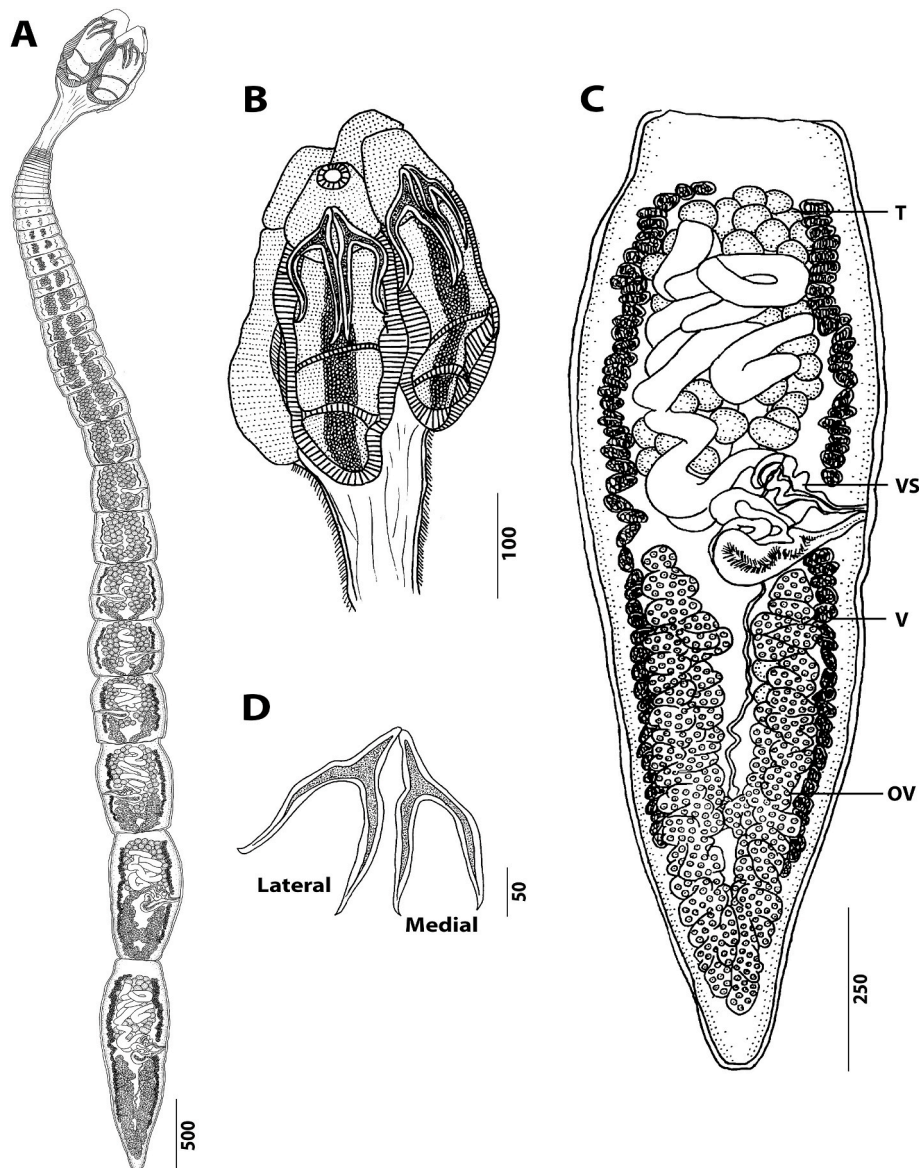
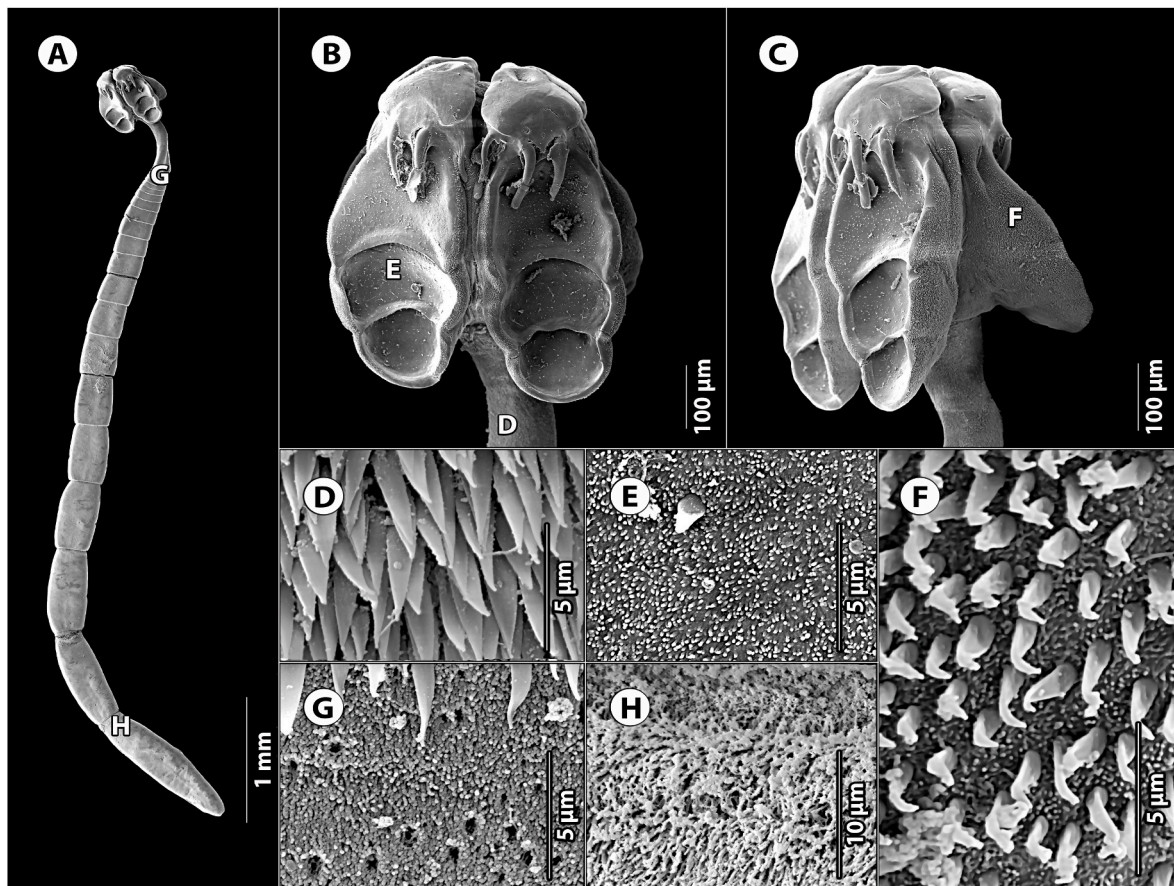


Fig. 3. Line drawings of *Acanthobothrium usengozinius* n. sp. A – entire specimen (holotype; accession no. XXX); B – scolex; C – mature proglottid (VS, vaginal sphincter; T, testis; V, vitelline follicle; OV, ovary); D – hooks.



**Fig. 4.** Scanning electron micrographs of *Acanthobothrium usengozinius* n. sp. **A** – entire specimen, letters indicate where micrographs of microtriches were taken; **B** – scolex, dorsoventral view, letter indicates where micrographs of microtriches were taken; **C** – scolex, lateral view, letter indicates where micrograph of microtriches was taken; **D** – cephalic peduncle; **E** – distal bothridial surface; **F** – proximal bothridial surface, near medial margin of bothridium; **G** – first proglottid; **H** – anterior region of terminal proglottid.

prominent (Fig. 3C). Ovary occupying about half of proglottid length, almost reaching posterior margin of proglottid, H-shaped in dorsoventral view, lobulated (Fig. 3C), asymmetrical, 143–180 wide at level of ovarian isthmus; poral lobe 548–679 in length; aporal lobe 616–757 in length; ovarian lobes not reaching cirrus-sac anteriorly; ovarian isthmus located posterior to mid-level of ovary. Mehlis' gland posterior to ovarian isthmus.

Vitellarium follicular to lobulated; follicles in two lateral bands, 27–35 long by 17–20 wide, length relative to testis length 0.4–0.6 : 1.0; each band consisting of two columns, extending from posterior margin of anterior-most testes to near posterior margin of ovary (Fig. 3C). Uterus thin-walled, extending from ovarian isthmus to near anterior margin of proglottid. Eggs not observed.

Type host: White skate, *Rostroraja alba* (Lacépède) (Rajiformes: Rajidae).

Type locality: Danger Point, Gansbaai, South Africa [34°28'50''S, 19°19'55''E].

Site of infection: Spiral intestine.

Prevalence of infection: 50% (one of two skates examined).

Type material: Holotype deposited at NMB (Accession number: XXX), paratypes in NMB (Accession numbers: XXX-XXX), IPCAS (Accession numbers: XXX-XXX) and MHNG (Accession numbers: XXX-XXX).

ZooBank number for species: XXXXXX.

**Etymology:** The species name “*usengozinius*” is derived from “*usengozini*” [Xhosa; an indigenous language to the Eastern and Western Cape of South Africa] meaning “endangered”, referring to the threatened status of both the definitive host *Rostroraja alba*, as well as its host-

specific parasite.

#### Remarks

*Acanthobothrium usengozinius* n. sp. is a category 2 species (sensu Ghoshroy and Caira, 2001). Similar to the description of *A. umbungus* n. sp., hooks of *A. usengozinius* n. sp. are the most prominent feature, instantly distinguishing it from all but five (i.e. *A. annapienkensis*, *A. brayi*, *A. domingae*, *A. guanghaiense* and *A. umbungus* n. sp.) of the 52 representatives within category 2. The remaining category 2 species present much smaller hook measurements than those of the new species, as follows: lateral hooks: *A* < 62 µm vs 62–73 µm, *B* < 130 µm vs 135–151 µm, *C* < 124 µm vs 129–141 µm, *D* < 178 µm vs 190–216 µm, respectively; medial hooks: *A'* < 64 µm vs 64–74 µm, *B'* < 136 µm vs 139–162 µm, *C'* < 122 µm vs 125–142 µm, *D'* < 193 µm vs 193–228 µm, respectively. The only species with larger hooks than *A. usengozinius* n. sp. is *A. annapienkensis* (lateral hooks *A* > 73 µm vs 62–73 µm, *B* > 180 µm vs 139–162 µm, *C* > 160 µm vs 125–142 µm, *D* > 240 µm vs 193–228 µm, respectively). Apart from hook measurements, *A. benedenii* Lönnberg, 1889, *A. bobconniorum*, *A. brachyacanthum*, *A. brayi*, *A. brevissime*, *A. campbelli*, *A. carolinae*, *A. chisholmae*, *A. dasi* Ghoshroy et Caira, 2001, *A. domingae*, *A. dujardini*, *A. edwardsi*, *A. gloveri*, *A. lasti*, *A. lilium*, *A. mashniae*, *A. michrohabentes*, *A. microtenuis*, *A. minus*, *A. mooreae*, *A. ocallaghani* Campbell et Beveridge, 2002, *A. olseni*, *A. ppdeleoni*, *A. rajivi*, *A. sinaloansis*, *A. sphaera*, *A. stevensi*, *A. tasajerasi*, *A. tetabuanense*, *A. thomasa*, *A. tripartitum*, *A. quadripartitum*, *A. vargasi*, *A. walkeri* and *A. zapteryum* can all be distinguished from *A. usengozinius* n. sp. by a much smaller body size (< 6 mm vs 6.3–8.8 mm, respectively),

whereas *A. urotrygoni* and *A. woodsholei* are significantly larger (>12 mm vs 6.3–8.8 mm, respectively). Additionally, *A. benedenii*, *A. bobconniorum*, *A. brachyacanthum*, *A. brevissime*, *A. campbelli*, *A. cimari*, *A. costaricense*, *A. crassus*, *A. dolichocollum*, *A. dujardini*, *A. edwardsi*, *A. hypanus*, *A. lasti*, *A. lilium*, *A. mashnihae*, *A. michrohabetes*, *A. microtenuis*, *A. minus*, *A. mooreae*, *A. ocallaghani*, *A. olseni*, *A. ppdeleoni*, *A. quadripartitum*, *A. semnovesiculum*, *A. sinaloansis*, *A. soniae*, *A. sphaera*, *A. stevensi*, *A. tasajerasi*, *A. tetabuanense*, *A. thomasa*, *A. umbungus* n. sp., *A. urotrygoni*, *A. vargasi*, *A. walkeri*, and *A. zapteryicum* show differences in the following features: scolex length (<540 µm vs 540–631 µm, respectively), bothridium width (<214 µm vs 215–245 µm, respectively), cephalic peduncle width (<115 µm vs 119–124 µm, respectively), and ovary width (<116 µm vs 143–180 µm, respectively). In comparison *A. annapienkensis*, *A. bullardi* and *A. woodsholei* all have a longer scolex (>633 µm vs 540–631 µm, respectively). The poral ovarian lobe of *A. bobconniorum*, *A. brachyacanthum*, *A. brayi*, *A. campbelli*, *A. carolinae*, *A. chisholmae*, *A. dasi*, *A. domingae*, *A. gloveri*, *A. guanghaiense*, *A. hypanus*, *A. lasti*, *A. mashnihae*, *A. michrohabetes*, *A. microtenuis*, *A. mooreae*, *A. ocallaghani*, *A. ppdeleoni*, *A. rajivi*, *A. sinaloansis*, *A. sphaera*, *A. stevensi*, *A. tasajerasi*, *A. tetabuanense*, *A. thomasa*, *A. urotrygoni*, *A. vargasi*, and *A. walkeri* are shorter than that of *A. usengozinius* n. sp. (<525 µm vs 548–679 µm, respectively). The same applies for the aporal lobe (<565 µm vs 616–757 µm, respectively). The following species all have a wider cirrus-sac than that of *A. usengozinius* n. sp. (>60 µm vs 43–57 µm): *A. annapienkensis*, *A. bobconniorum*, *A. brachyacanthum*, *A. brayi*, *A. bullardi*, *A. costaricense*, *A. dolichocollum*, *A. domingae*, *A. mooreae*, *A. olseni*, *A. popi*, *A. ppdeleoni*, *A. rajivi*, *A. semnovesiculum*, *A. soniae*, *A. thomasa* and *A. urotrygoni*. *Acanthobothrium cimari*, *A. costaricense*, *A. crassus*, *A. dolichocollum*, *A. guanghaiense*, *A. hypanus*, *A. puntarenasense*, *A. semnovesiculum* and *A. soniae* also differ from *A. usengozinius* n. sp. in a number of features such as: a narrower bothridium (<214 µm vs 215–245 µm, respectively), a shorter anterior loculus (<205 µm vs 235–257 µm, respectively), a shorter middle loculus (<90 µm vs 126–143 µm, respectively), a shorter posterior loculus (<91 µm vs 94–106 µm, respectively), and a narrower ovary (<120 µm vs 143–180 µm, respectively).

*Acanthobothrium usengozinius* n. sp. marks the fourth species described from the endangered host, *R. alba*, expanding the remarkable host specificity within the genus. This discovery therefore subsequently marks the importance of dedicating appropriate research to endangered elasmobranch species, as macrohabitats of numerous parasitic organisms new to science that are threatened by co-extinction. *Acanthobothrium usengozinius* n. sp. also marks the sixth species of this genus from the Eastern South Atlantic Ocean.

### 3.4. *Acanthobothrium ulondolozus* n. sp. (Figs. 5 and 6)

**Description** (based on whole mounts of seven mature worms; two mature worms examined with SEM): Worms 9.3–13.5 mm long, greatest width at level of scolex, 32–50 proglottids per worm, euapolytic. Scolex consisting of scolex proper and cephalic peduncle. Scolex proper with four bothridia, 486–599 long by 324–520 wide. Bothridia free posteriorly, 168–190 wide; each bothridium with three loculi and specialised anterior region in form of muscular pad. Muscular pad 128–150 long by 146–162 wide, falciform in shape, with pronounced posterior margin, bearing accessory sucker and one pair of hooks at posterior margin; accessory sucker 27–37 long by 35–48 wide. Anterior loculus (A) 201–212 long; middle loculus (M) 72–120 long; posterior loculus (P) 97–113 long; loculus length ratio (A: M: P) 1.00 : 0.53: 0.52; maximum width of scolex at level of middle loculus. Velum absent.

Hooks bi-pronged, hollow, with tubercle on proximal surface of axial prongs; internal channels of axial and abaxial prongs continuous, smooth; axial prongs slightly longer than abaxial prongs; lateral and medial hooks approximately equal in size. Lateral hook measurements: A 60–75, B 154–160, C 131–144, D 212–220. Medial hook measurements: A' 62–73, B' 144–165, C' 121–144, D' 203–211. Bases of lateral

and medial hooks approximately equal in length; base of medial hook slightly overlapping base of lateral hook along medial axis of bothridium (Fig. 5D); medial hook base slightly wider than lateral hook base. Tissue covering almost entire length of each prong of hooks. Short cephalic peduncle 1044–1430 long by 76–98 wide.

Cephalic peduncle densely covered with gladiate spinitriches, filitriches not observed (Fig. 6C). Apical pad and distal bothridial surface covered with papilliform to acicular filitriches and extremely sparsely interspersed gladiate spinitriches (Fig. 6D). Proximal bothridial surface and bothridial rims covered with gladiate spinitriches, interspersed with acicular filitriches (Fig. 6E). Anterior region of strobila covered in acicular filitriches (Fig. 6F). Anterior region of terminal proglottid covered in capilliform filitriches (Fig. 6G).

Proglottids acraspedote. Immature proglottids 29–48 in number; 2–3 mature proglottids; gravid proglottids absent; terminal proglottid 1063–2134 long by 284–356 wide; terminal proglottid length to width ratio 3.2–6.3 : 1.0. Proglottids protandrous; genital pores marginal, irregularly alternating (Fig. 5A), 48–59% of proglottid length from posterior margin.

Testes conspicuous in mature proglottids, oval in dorsoventral view, 50–61 long by 40–52 wide, arranged in one to two layers in intervascular field (Fig. 5C), 50–62 in total number, 8–9 in post-poral field; some segments with single testis posterior to ovarian isthmus. Cirrus-sac J-shaped, tilted posteriorly (Fig. 5C), 171–232 long by 60–73 wide, containing armed cirrus; cirrus greatly expanded at base.

Vagina narrow, relatively thin-walled and straight proximally, extending from ootype along medial line of proglottid to anterior margin of cirrus-sac, then laterally to common genital atrium. Vaginal sphincter prominent (Fig. 5C). Ovary occupying about half of proglottid length, almost reaching posterior margin of proglottid, H-shaped in dorsoventral view, lobulated (Fig. 5C), asymmetrical, 107–149 wide at level of ovarian isthmus; poral lobe 431–981 in length; aporal lobe 503–1133 in length; ovarian lobes not reaching cirrus-sac anteriorly; ovarian isthmus located posterior to mid-level of ovary. Mehlis' gland posterior to ovarian isthmus.

Vitellarium follicular to lobulated; follicles in two lateral bands, 13–21 long by 23–43 wide, length relative to testis length 0.2–0.4 : 1.0; each band consisting of two columns, extending from posterior margin of anterior-most testes to near posterior margin of ovary (Fig. 5C). Vitelline follicle length relative to testis length 0.2–0.4 : 1.0. Uterus thin-walled, extending from ovarian isthmus to near anterior margin of proglottid. Eggs not observed.

Type host: White skate, *Rostroraja alba* (Lacépède) (Rajiformes: Rajidae).

Type locality: Danger Point, Gansbaai, South Africa [34°28'50''S, 19°19'55''E].

Site of infection: Spiral intestine.

Prevalence of infection: 50% (one of two skates examined).

Type material: Holotype deposited at NMB (Accession number: XXX), paratypes in NMB (Accession numbers: XXX-XXX), IPCAS (Accession numbers: XXX-XXX) and MHNG (Accession numbers: XXX-XXX).

ZooBank number for species: XXXXXX.

**Etyymology:** The species name “*ulondolozus*” is derived from “ulondolozo” [Xhosa; an indigenous language to the Eastern and Western Cape of South Africa] meaning “conservation”, referring to the need for having better conservation plans for threatened elasmobranch species, which would also protect a wide variety of host-specific affiliate species facing an increased risk of co-extinction.

### Remarks

All of the new species described in the present study seem most distinguishable by their hooks. Just as *Acanthobothrium umbungus* n. sp. and *A. usengozinius* n. sp., *A. ulondolozus* n. sp. is identified as a category 2 species. However, unlike the two new congeners, *A. ulondolozus* n. sp.

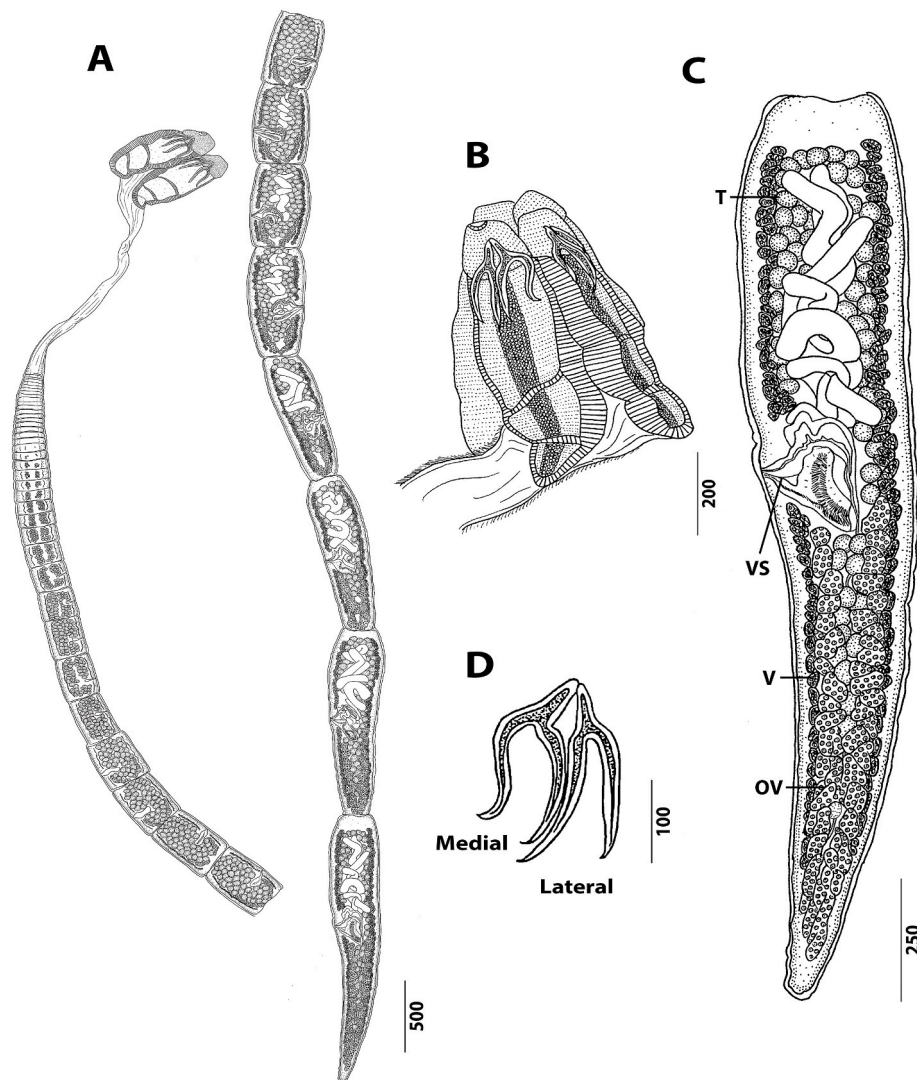


**Fig. 5.** Line drawings of *Acanthobothrium ulondolozus* n. sp. **A** – entire specimen (holotype; accession no. XXX); **B** – scolex; **C** – mature proglottid (VS, vaginal sphincter; T, testis; V, vitelline follicle; OV, ovary); **D** – hooks.

is the only species in the present study with occasional testes posterior to the ovarian isthmus. This is still regarded as an exceptional feature among species of *Acanthobothrium*, being present in less than 10% of all species recognised within this genus worldwide. Hence, *A. ulondolozus* n. sp. can easily be distinguished from all but 16 congeners (across all categories). From the remaining 16 species of *Acanthobothrium* known to bear this feature, only six are identified as category 2 species, namely *A. bobconniorum*, *A. crassus*, *A. dolichocollum*, *A. microhabentes*, *A. microtenuis*, and *A. popi*. *Acanthobothrium microhabentes* and *A. microtenuis* were only recently described from the same biogeographical region by Van Der Spuy et al. (2020). However, both species differ from *A. ulondolozus* n. sp. in smaller metrical features (i.e. total length, scolex length, scolex width, bothridium width, lateral hooks, medial hooks, cephalic peduncle width, cirrus-sac length, poral and aporal ovarian length, ovarian width; see Van Der Spuy et al., 2020), while *A. bobconniorum*, *A. crassus*, *A. dolichocollum* and *A. popi* differ from *A. ulondolozus* n. sp. in the following features: smaller lateral hooks ( $A < 60 \mu\text{m}$  vs  $60\text{--}75 \mu\text{m}$ ,  $B < 120 \mu\text{m}$  vs  $154\text{--}160 \mu\text{m}$ ,  $C < 100 \mu\text{m}$  vs  $131\text{--}144 \mu\text{m}$ ,  $D < 175 \mu\text{m}$  vs  $212\text{--}220 \mu\text{m}$ , respectively), smaller medial hooks ( $A' < 60 \mu\text{m}$  vs  $62\text{--}73 \mu\text{m}$ ,  $B' < 119 \mu\text{m}$  vs  $144\text{--}165 \mu\text{m}$ ,  $C' < 108 \mu\text{m}$  vs  $121\text{--}144 \mu\text{m}$ ,  $D' < 175 \mu\text{m}$  vs  $203\text{--}211 \mu\text{m}$ , respectively), a shorter terminal proglottid ( $< 1320 \mu\text{m}$  vs  $1663\text{--}2134 \mu\text{m}$ , respectively), a narrower terminal proglottid ( $< 260 \mu\text{m}$  vs  $284\text{--}356 \mu\text{m}$ , respectively), a

shorter cirrus-sac ( $< 152 \mu\text{m}$  vs  $171\text{--}232 \mu\text{m}$ , respectively) and smaller testes ( $< 50 \mu\text{m}$  vs  $50\text{--}61 \mu\text{m}$ , respectively). Furthermore, *A. bobconniorum* and *A. popi* differ from *A. ulondolozus* n. sp. in the following features: total length ( $< 7.1 \text{ mm}$  vs  $9.3\text{--}13.5 \text{ mm}$ , respectively), cephalic peduncle length ( $< 650 \mu\text{m}$  vs  $1044\text{--}1430 \mu\text{m}$ , respectively), and testes length ( $< 50 \mu\text{m}$  vs  $50\text{--}61 \mu\text{m}$ , respectively). Both *A. crassus* and *A. dolichocollum* have a shorter scolex than *A. ulondolozus* n. sp. ( $< 450 \mu\text{m}$  vs  $486\text{--}599 \mu\text{m}$ , respectively). Additionally, the width of both the bothridium and cephalic peduncle can also be used to distinguish *A. ulondolozus* n. sp. from *A. dolichocollum*, as the latter species has a narrower bothridium ( $< 134 \mu\text{m}$  vs  $168\text{--}190 \mu\text{m}$ , respectively), and a narrower cephalic peduncle ( $< 73 \mu\text{m}$  vs  $76\text{--}98 \mu\text{m}$ , respectively).

Species of *Acanthobothrium* possessing testes posterior to the ovarian isthmus seem to be restricted to the families Dasyatidae (i.e. *Himantura* Müller et Henle), Rhinidae (i.e. *Rhynchobatus* Müller et Henle), Rhinobatidae (i.e. *Rhinobatos* Linck) and Rajidae (i.e. *Raja* Linnaeus), with the latter family including the host observed in the present study. The addition of yet another South African congener, *A. ulondolozus* n. sp., not only brings the total of species known to possess this remarkable feature to 17 species (across all categories), but also subsequently confirms Van Der Spuy et al.'s (2020) statement that this feature is not limited to the Indo-Pacific Ocean. Moreover, the plausibility regarding the relatedness of *A. ulondolozus* n. sp. with other congeners only invites further

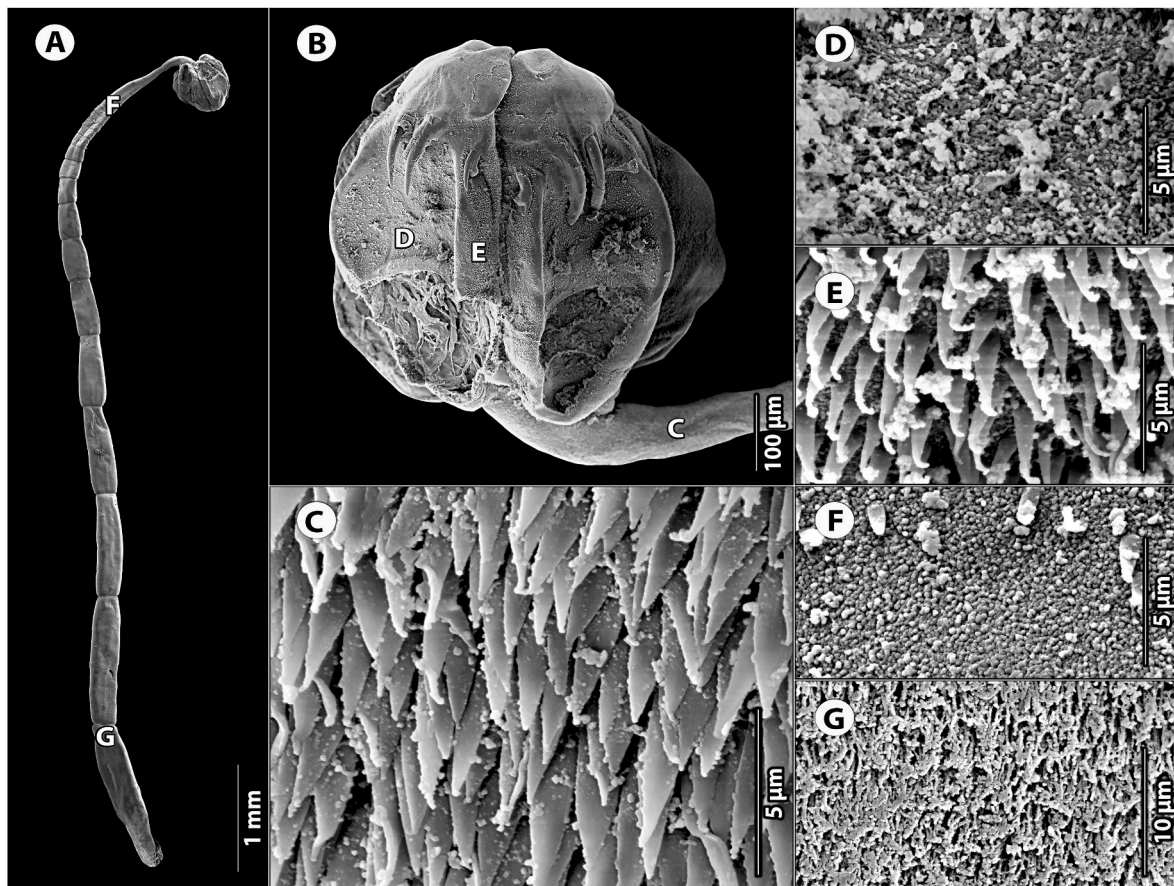


**Fig. 6.** Scanning electron micrographs of *Acanthobothrium ulondolozus* n. sp. **A** – entire specimen, letters indicate where micrographs of microtriches were taken; **B** – scolex, letters indicate where micrographs of microtriches were taken; **C** – cephalic peduncle; **D** – distal bothridial surface; **E** – proximal bothridial surface, near medial margin of bothridium; **F** – first proglottid; **G** – anterior region of terminal proglottid.

research engagement. The fact that *A. ulondolozus* n. sp. is synhostalitic with two other congeners and sharing a rare morphological feature with only 16 other species of *Acanthobothrium* worldwide (i.e. four from South Africa), further supports the need for future research into a more comprehensive phylogenetic analysis of these cestodes. Gathering information on the molecular phylogeny could prove if species presenting testes located in this region might in fact comprise their own monophyletic clade (Fyler and Caira, 2010), along with possible effects caused by regional geographical influences (i.e. the Eastern South Atlantic Ocean vs. the Indo-Pacific Ocean), given that adult species of *Acanthobothrium* are restricted to the same geographical limits portrayed by their hosts (Zaragoza-Tapia et al., 2020a).

*Acanthobothrium ulondolozus* n. sp. is the fifth cestode species known to parasitise the endangered white skate, *R. alba*, and the first cestode species infecting this host bearing testes posterior to the ovarian isthmus. This adds *R. alba* to the list of elasmobranch species known to host species of *Acanthobothrium* with this particularly rare morphological feature. Furthermore, *A. ulondolozus* n. sp. represents the seventh species known from the southeastern Atlantic Ocean off the coast of southern Africa, and the fifth species from this region with testes posterior to the ovarian isthmus, a feature previously thought to be restricted to the Indo-Pacific Ocean (Fyler et al., 2009; Fyler and Caira, 2010; Maleki et al., 2015).

#### 4. Discussion

Cestodes constitute the most biodiverse metazoan parasite group infecting elasmobranchs worldwide (Caira and Healy, 2004). They fulfil vital roles in trophic systems and the health of a marine ecosystem,

subsequently rendering them indispensable in ensuring healthy and more resilient marine ecosystems (Beer et al., 2019). However, researchers only dedicate limited attention to this group, leaving large gaps in taxonomic, biological, and ecological research as well as species conservation efforts (Caira and Healy, 2004; Poulin and Presswell, 2016; Randhawa and Poulin, 2020). With merely 40% of all known elasmobranch species examined for cestode infections (Caira and Jensen, 2017), parasitological research efforts have been extremely sparse in many hosts and regions of the world. This is grounded upon the fact that many research initiatives are greatly biased towards individual, more acknowledged elasmobranch host groups (Poulin and Presswell, 2016), and exacerbated by limited financial means and research expertise in specific regions, which are occupied by many endemic organisms with narrow geographical ranges (Randhawa et al., 2015; Randhawa and Poulin, 2020). This is especially true for biogeographical regions surrounding the South-eastern Atlantic Ocean.

The ocean basins surrounding Southern Africa present a high diversity of elasmobranch host species (Ebert and van Hees, 2015). However, only 19 out of 204 elasmobranch species (i.e. 9 % of the species diversity) reported from Southern Africa have been observed for parasites (Schaeffner and Smit, 2019; Van Der Spuy et al., 2020). Given that each elasmobranch species hosts several unique cestode species (Caira and Healy, 2004; Schaeffner and Smit, 2019), there is little doubt that future parasitological studies will reveal an immense hidden diversity of parasitic organisms, particularly cestodes, in this host group. This, in turn, might strengthen the conservation of large, apex-predator species and their numerous affiliated species, and ultimately the preservation of threatened host-parasite systems.

The present study describes three, host-specific species of

onchoproteocephalidean cestodes of the genus *Acanthobothrium*. Merely 7% (16 of 207) of all species of this genus have been reported from this region (see Zaragoza-Tapia et al., 2020a). The new species from South Africa further increase the diversity of this already very diverse genus, with a new total of 210 valid species worldwide (Caira and Jensen, 2017; Franzese and Ivanov, 2018, 2020; Maleki et al., 2018, 2019; Rodríguez-Ibarra et al., 2018; Zaragoza-Tapia et al., 2019, 2020b; Van Der Spuy et al., 2020). Unfortunately, as a result of observing a limited number of specimens from an endangered host species, no specimens were recovered from ethanol-fixed material in order to conduct a proper molecular analysis. For this reason, the phylogenetic relationships of these congeners are presently unknown. Globally, there is still a great shortfall in molecular data regarding species belonging to this genus, supported by the fact that the GenBank database contain molecular sequences and records of merely 7.6% (16 of 210) of species of *Acanthobothrium* (Zaragoza-Tapia et al., 2020a). The information gained through phylogenetic analyses will not only address phylogenetic placement of parasite lineages, but further advance our knowledge on evolutionary host-parasite interrelationships, along with host-parasite co-speciation (Beer et al., 2019), and relevant niche expertise (Zaragoza-Tapia et al., 2020a).

The species described herein were recovered from an endangered host species, the white skate, *R. alba*. Apart from the alarming fact that this species is listed in the second-highest category in the International Union for Conservation of Nature's (IUCN) Red List of Threatened Species, with major implications on the conservation status and future conservation efforts of its affiliated (and host-specific parasite) species, it is a prime example that demands further research, contributing essential, valuable insights regarding deficient ecological data (Sousa et al., 2019). This study marks the first parasitological observation of this species in a different biogeographic region along its distributional range and the first from Southern Africa. Prior to this study, this endangered species has been sparsely screened for cestode parasites, exclusively under its former name *Raja marginata* Lacepède, 1803 and material collected in the Mediterranean Sea (see Baer, 1948; Euzet et al., 1959; Goldstein, 1967; Williams, 1969; Zaragoza-Tapia et al., 2020a). At present, only six, valid species of cestodes were reported from this host along its entire distributional range, including one diphyllidean species, *Echinobothrium affine* Diesing, 1863 (see Tyler, 2006), and three rhinebothriideans, namely *Echeneibothrium demeusiae* Euzet et al., 1959, *E. dubium* van Beneden, 1850, and *E. variabile* van Beneden (1850) (see Euzet et al., 1959). Only two additional species of *Acanthobothrium* were recorded from *R. alba*, *Acanthobothrium filicolle* (Zschokke, 1888) Yamaguti, 1959 and *A. rajaebatis* (Rudolphi, 1810) Euzet et al., 1959, both from *R. alba* (as *R. marginata*) from the Mediterranean Sea off France (Baer, 1948; Euzet et al., 1959). Although these species have been recorded from the same host species as *A. umbungus* n. sp., they originate from a different biogeographical region than the present specimens and furthermore fall into different categories of Ghoshroy and Caira (2001) classification system. Following Ghoshroy and Caira (2001) system, *A. filicolle* represents a category 1 species, with a body size <15 mm (i.e. 6–8 mm in Baer, 1948), <50 segments (i.e. 17 to 30 in Baer, 1948), <80 testes (i.e. 30 to 40 in Baer, 1948; 24 to 56 in Euzet et al., 1959) and a symmetrical ovary (see illustrations in Baer, 1948 and Euzet et al., 1959). *Acanthobothrium rajaebatis* most likely represents a category 5 species, with a total length of 50–60 mm (see Euzet et al., 1959), >80 segments (i.e. 80 to 120 in Goldstein, 1967; more than 100 in Williams, 1969), between 58 and 85 testes (i.e. with a mean of 72 in Euzet et al., 1959), and a symmetrical ovary (see Goldstein, 1967 and illustration in Euzet et al., 1959). Yet, values for the number of testes superimpose the boundary of 80 testes of Ghoshroy and Caira (2001) system, which could also place this species into category 4. The placement of both congeners in different categories automatically excluded them from the species differentiations (above).

Species of *Acanthobothrium* are synhospitalic, possibly as a result of host-substitution events due to geographical and external environmental

conditions (Fyler, 2009), causing lineage sorting, providing evidence of co-speciation (Beer et al., 2019), and therefore exhibiting an extraordinary specificity towards both their elasmobranch hosts as well as their environmental requirements (Nhi et al., 2013). By understanding the ecological importance of co-speciation events along with ecological factors, such as the hosts' specific diet, size, geographical location and depth, which ultimately shapes host-parasite systems, researchers might have a better chance of mitigating co-extinction events in the future (Beer et al., 2019). However, given the decline in host populations and steady increase in the number of threatened species, co-extinction events grow more and more likely, although unnoticed, leading to the loss of many parasites, or better affiliate species, including a vast number of yet undescribed species (Davidson and Dulvy, 2017). These co-extinctions might trigger a series of long-term and indirect negative effects, leaving detrimental repercussions, which are currently not fully understood.

The discovery of additional species of *Acanthobothrium* will, without a doubt, be beneficial in this regard, as genera with a higher parasite species diversity can be more sustainably used as biological and ecological indicators of their elasmobranch hosts' life conditions, aiding the conservation of specific host populations (Marcogliese, 2005; Nhi et al., 2013). These cestodes could play a vital role in ecosystem health assessments, when considered suitable indicators of pollution or other environmental changes on host species. Certain cestode species are able to accumulate pollutants such as heavy metals from their specific host tissues at high concentrations, possibly lowering the effects of these pollutants for vulnerable host species (Jankovská et al., 2011; Nhi et al., 2013). These parasites will therefore provide valuable insights to the vulnerability of specific host species, whereas understanding the host-parasite system may be just as vital providing insights to the vulnerability of the parasites to co-extinction with their host species (Beer et al., 2019).

Extensive studies on elasmobranch parasites and their hosts implementing multisource approaches (e.g., taxonomy, molecular systematics, biogeography, ecology, ecotoxicology) are needed, in order to provide a better understanding on the intimate nature of this particular and ancient host-parasite system. This may ultimately lead to new prospects in conservation science and the preservation of threatened host species, such as *R. alba*, together with their unique parasite fauna. Furthermore, the conservation of endangered species, such as *R. alba*, harbouring cestode parasites is crucial to mitigate host-parasite co-extinction events, whereby conservation of the parasite species along with its host, contributes to the conservation of marine ecosystem, rather than merely a single species. Since these affiliate species provide numerous positive attributes to hosts and environment, which rely on their elasmobranch hosts as macroenvironments, they deserve consideration in modern conservation schemes. The incorporation of such affiliates in future conservation agendas is crucial and greatly encouraged, as the absence of these species in the "ecological theatre" (sensu Marcogliese, 2004) as well as on-going evolutionary processes, will be profoundly altered once extinction and co-extinction events occur.

## Declaration of funding

This work was supported by both a Foundational Biodiversity Information Programme of the National Research Foundation (FBIP-NRF) of South Africa masters bursary of LVDS (UID 128316), as well as an NWU postdoctoral fellowship of BCS. Opinions, findings, conclusions and recommendations expressed in this publication are that of the authors, and the NRF accept no liability whatsoever in this regard.

## Data availability status

The data used to generate the results in the paper are available and can be accessed by contacting the corresponding author. Species registration details can be accessed by the various zoobank links provided.

## Declaration of competing interest

The authors declare no conflicts of interest.

## Acknowledgements

We are very grateful to the members of the South African Shark Conservancy for their collaboration and assistance in the field, especially Megan McCord, Björn von Düring, Natalia Drobniewska and Guy Paulet. We would also like to thank the Unit for Environmental Sciences and Management, North-West University (NWU) for the use of field equipment and laboratory facilities. Additional thanks go to our colleagues Ruan Gerber, Chantelle Pretorius, and Rian Pienaar from the NWU-Water Research Group who assisted with collection of samples. This is contribution No. XXX from the NWU-Water Research Group.

## References

- Baer, J.G., 1948. Contributions a l'étude des cestodes de sélaciens I-IV. *Bull. Soc. Neuchl. Sci. Nat.* 71, 63–122.
- Baer, J.G., Euzet, L., 1962. Revision critique des Cestodes Tétraphyllides décrits par T. Southwell. *Bull. Soc. Neuchl. Sci. Nat.* 85, 143–172.
- Beer, A., Ingram, T., Randhawa, H.S., 2019. Role of ecology and phylogeny in determining tapeworm assemblages in skates (Rajiformes). *J. Helminthol.* 93, 738–751.
- Brooks, D.R., 1977. Six new species of tetraphyllidean cestodes, including a new genus, from a marine stingray *Himantura schmardae* (Werner, 1904) from Colombia. *Proc. Helminthol. Soc. Wash.* 44, 51–59.
- Brooks, D.R., Mayes, M.A., 1980. Cestodes in four species of euryhaline stingrays from Colombia. *Proc. Helminthol. Soc. Wash.* 47, 22–29.
- Caira, J.N., Healy, C.J., 2004. Elasmobranchs as hosts of metazoan parasites. In: Carrier, J.C., Musick, J.A., Heithaus, M.R. (Eds.), *Biology of Sharks and Their Relatives*. CRC Press, Boca Raton, FL, USA, pp. 523–551.
- Caira, J.N., Jensen, K., 2001. An investigation of the co-evolutionary relationships between onchobothriid tapeworms and their elasmobranch hosts. *Int. J. Parasitol.* 31, 960–975.
- Caira, J.N., Jensen, K., 2014. A digest of elasmobranch tapeworms. *J. Parasitol.* 100, 373–391.
- Caira, J.N., Jensen, K. (Eds.), 2017. *Planetary Biodiversity Inventory (2008–2017): Tapeworms from Vertebrate Bowels of the Earth*. The University of Kansas Natural History Museum, Special Publication no. 25, Lawrence, p. 463.
- Campbell, R.A., Beveridge, I., 2002. The genus *Acanthobothrium* (Cestoda: Tetracyphillidae: Onchobothriidae) parasitic in Australian elasmobranch fishes. *Invertebr. Systemat.* 16, 273–344.
- Carvajal, G.J., Goldstein, R.J., 1971. *Acanthobothrium annapinkiensis* n. sp. (Cestoda: Tetracyphillidae: Onchobothriidae) from the skate, *Raja chilensis* (Chondrichthyes: Rajiidae) from Chile. *Zool. Anz.* 186, 158–162.
- Dailey, M.D., Mudry, D.R., 1968. Two new species of cestodes from California rays. *J. Parasitol.* 54, 1141–1143.
- Davidson, L.N.K., Dulvy, N.K., 2017. Global marine protected areas to prevent extinctions. *Nat. Ecol. Evol.* 1, 0040.
- Dentzien-Dias, P.C., Poinar Jr., G., de Figueiredo, A.E.Q., Pacheco, A.C.L., Horn, B.L.D., Schultz, C.L., 2013. Tapeworm Eggs in a 270 Million-year-Old Shark Coprolite. *PLoS One* 8, e55007.
- Ebert, D., van Hees, K.E., 2015. Beyond jaws: rediscovering the 'lost sharks' of southern Africa. *Afr. J. Mar. Sci.* 37, 141–156.
- Euzet, L., 1959. *Recherches sur les cestodes tétraphyllides des sélaciens des côtes de France*. Doctoral Dissertation, Université de Montpellier, p. 263. Montpellier.
- Franzese, S., Ivanov, V.A., 2018. Hyperapolytic species of *Acanthobothrium* (Cestoda: Onchoproteocephalidae) from batoids off Argentina. *Parasitol. Int.* 67, 431–443.
- Franzese, S., Ivanov, V.A., 2020. Two new species of *Acanthobothrium* Blanchard, 1848 (Cestoda: Onchoproteocephalidae) from rajiform batoids off Argentina. *Folia Parasitol.* 67, 016.
- Fyler, C.A., 2009. *Systematics, Biogeography and Character Evolution in the Tapeworm Genus Acanthobothrium Van Beneden, 1850*. ProQuest Dissertations Publishing, University of Connecticut, p. 200.
- Fyler, C.A., Caira, J.N., 2006. Five new species of *Acanthobothrium* (Tetracyphillidae: Onchobothriidae) from the freshwater stingray *Himantura chaophraya* (Batoidea: Dasyatidae) in Malaysian Borneo. *J. Parasitol.* 92, 105–125.
- Fyler, C.A., Caira, J.N., 2010. Phylogenetic status of four new species of *Acanthobothrium* (Cestoda: Tetracyphillidae) parasitic on the wedge fish *Rhynchobatus laevis* (Elasmobranchii: Rhynchobatidae): implications for interpreting host associations. *Invertebr. Systemat.* 24, 419–433.
- Fyler, C.A., Caira, J.N., Jensen, K., 2009. Five new species of *Acanthobothrium* (Cestoda: Tetracyphillidae) from an unusual species of *Himantura* (Rajiformes: Dasyatidae) from northern Australia. *Folia Parasitol.* 56, 107–128.
- Ghoshroy, S., Caira, J.N., 2001. Four new species of *Acanthobothrium* (Cestoda: Tetracyphillidae) from the whiptail stingray *Dasyatis brevis* in the Gulf of California, Mexico. *J. Parasitol.* 87, 354–372.
- Goldstein, R.J., 1967. The genus *Acanthobothrium* van Beneden, 1849 (Cestoda: Tetracyphillidae). *J. Parasitol.* 53, 455–483.
- IUCN, 2021. The IUCN Red List of Threatened Species. <http://www.iucnredlist.org>. (Accessed 23 June 2021).
- Jankovská, I., Mihalová, D., Petrář, M., Romocuský, S., Kalous, L., Vadlejch, J., Cadková, Z., Langrová, L., 2011. The intestinal parasite *Acanthocephalus lucii* (Acanthocephala) from European perch (*Perca fluviatilis*) as a bioindicator for lead pollution in the stream "Jevanský potok" near Prague, Czech Republic. *Bull. Environ. Contam. Toxicol.* 86, 342–346.
- Linton, E., 1908. Helminth fauna of the dry Tortugas. I. Cestodes. In: *Papers from the Tortugas Laboratory*. Carnegie Institution of Washington, Washington, D.C., pp. 157–190.
- Lönnberg, E., 1889. Bidrag till Kanendomen om i Sverige förs Kommande cestoder. Bihang till Kongl. K. Sven. vetensk.akad. handl. 14, 1–69.
- Maleki, L., Malek, M., Palm, H.W., 2013. Two new species of *Acanthobothrium* (Tetracyphillidae: Onchobothriidae) from *Pastinachus cf. sephen* (Myliobatiformes: Dasyatidae) from the Persian Gulf and Gulf of Oman. *Folia Parasitol.* 60, 448–456.
- Maleki, L., Malek, M., Palm, H.W., 2015. Four new species of *Acanthobothrium* van Beneden, 1850 (Cestoda: Onchoproteocephalidae) from the guitarfish, *Rhynchobatus cf. djiddensis* (Elasmobranchii: Rhynchobatidae), from the Persian Gulf and Gulf of Oman. *Folia Parasitol.* 62, 012.
- Maleki, L., Malek, M., Palm, H.W., 2019. Five new species of *Acanthobothrium* (Cestoda: Onchoproteocephalidae) from the long-tailed butterfly ray, *Gymnura cf. poecilura* (Elasmobranchii: Gymnuridae), from the Persian Gulf and Gulf of Oman. *Zootaxa* 4609, 289–307.
- Maleki, L., Malek, M., Rastgoo, A., 2018. *Acanthobothrium chabahariensis* n. sp. (Cestoda: Onchoproteocephalidae) in the cownail stingray *Pastinachus cf. sephen* (Myliobatiformes: Dasyatidae) from the Gulf of Oman, Iran. *J. Genet. Res.* 4, 114–121.
- Marcogliese, D.J., 2004. Parasites: small players with crucial roles in the ecological theatre. *EcoHealth* 1, 151–164.
- Marcogliese, D.J., 2005. Parasites of the superorganism: are they indicators of ecosystem health? *Int. J. Parasitol.* 35, 705–716.
- Marques, F., Brooks, D.R., Monks, S., 1995. Five new species of *Acanthobothrium* van Beneden, 1849 (Eucestoda: Tetracyphillidae: Onchobothriidae) in stingrays from the Gulf of Nicoya, Costa Rica. *J. Parasitol.* 81, 942–951.
- Nhi, T.T.Y., Shazili, N.A.M., Harrison, F.S., 2013. Use of cestodes as indicator of heavy-metal pollution. *Exp. Parasitol.* 133, 75–79.
- Ostrowski de Núñez, M., 1971. Estudios preliminares sobre la fauna parasitaria de algunos elasmobranchios del litoral bonaerense, mar del plata, Argentina I. Cestodes y trematodes de *Psammobatis microps* (Gunther) y *Zapteryx brevirostris* (Muller Y Henle). *Physics* 30, 425–446.
- Poulin, R., Presswell, B., 2016. Taxonomic quality of species descriptions varies over time and with the number of authors, but unevenly among parasite taxa. *Syst. Biol.* 65, 1107–1116.
- Randhawa, H.S., Poulin, R., Krkosek, M., 2015. Increasing rate of species discovery in sharks coincides with sharp population declines: implications for biodiversity. *Ecography* 38, 96–107.
- Randhawa, H.S., Poulin, R., 2020. Tapeworm discovery in elasmobranch fishes: quantifying patterns and identifying their correlates. *Mar. Freshw. Res.* 71, 78–88.
- Reyda, F.B., Caira, J.N., 2006. Five new species of *Acanthobothrium* (Cestoda: Tetracyphillidae) from *Himantura uarnacoides* (Myliobatiformes: Dasyatidae) in Malaysian Borneo. *Comp. Parasitol.* 73, 49–71.
- Riser, N.W., 1955. Studies on cestode parasites of sharks and skates. *J. Tenn. Acad. Sci.* 30, 265–311.
- Rodríguez-Ibarra, E., Pulido-Flores, G., Violante González, J., Monks, S., 2018. A new species of *Acanthobothrium* (Eucestoda: Onchobothriidae) in *Aetobatus cf. narinari* (Myliobatidae) from Campeche, México. *Rev. Bras. Parasitol. Vet.* 27, 66–73.
- Schaeffner, B.C., Smit, N.J., 2019. Parasites of cartilaginous fishes (Chondrichthyes) in South Africa - a neglected field of marine science. *Folia Parasitol.* 66, 002.
- Siskey, M.R., Shipley, O.N., Frisk, M.G., 2019. Skating on thin ice: identifying the need for species-specific data and defined migration ecology of Rajidae spp. *Fish Fish.* 20, 286–302.
- Sousa, I., Baeyaert, J., Gonçalves, J.M.S., Erzini, K., 2019. Preliminary insights into the spatial ecology and movement patterns of a regionally critically endangered skate (*Rostroraja alba*) associated with a marine protected area. *Mar. Freshw. Behav. Physiol.* 52, 283–299.
- Sures, B., Nachev, M., Selbach, C., Marcogliese, D.J., 2017. Parasite responses to pollution: what we know and where we go in 'Environmental Parasitology. *Parasites Vectors* 10, 65.
- Tazerouti, F., Kechemir-Issad, N., Euzet, L., 2009. *Acanthobothrium minus* n. sp. (Tetracyphillidae: Onchobothriidae) parasite de *Raja asterias* (Elasmobranchii: Rajidae) en Méditerranée. *Parasite* 16, 203–207.
- Tyler, G.A., 2006. Tapeworms of elasmobranchs (Part III). A monograph on the Diphyllidae (Platyhelminthes, Cestoda). *Bull. Univ. Nebr. State Mus.* 20, 1–142.
- van Beneden, P.J., 1850. *Recherches sur la faune littorale de Belgique. Les vers cestodés, considérés sous le rapport physiologique, embryogénique et zooclassique*. *Mem. Acad. r. Sci. Lett. Belg.* 25, 1–204.
- Van Der Spuy, L., Smit, N.J., Schaeffner, B.C., 2020. Four new species of *Acanthobothrium* van Beneden, 1849 (Cestoda: Onchoproteocephalidae) from the spotted skate, *Raja straeleni* Poll, off the Western Cape, South Africa. *Folia Parasitol.* 67, 036.
- Verma, S.C., 1928. Some cestodes from Indian fishes including four new species of Tetracyphillidae and revised keys to the genera *Acanthobothrium* and *Gangesia*. *Univ. Allahabad Stud.* 4, 119–176.
- Williams, H.H., 1968. *Acanthobothrium quadripartitum* n. sp. (Cestoda: Tetracyphillidae) from *Raja naevus* in the North Sea and English channel. *Parasitology* 58, 105–110.
- Williams, H.H., 1969. The genus *Acanthobothrium* van Beneden 1849 (Cestoda: Tetracyphillidae). *Nytt Magasin Zool.* 17, 1–56.

- Yang, C., Sun, Y., Zhi, T., Iwaki, T., Reyda, F.B., Yang, T., 2016. Two new and one redescribed species of *Acanthobothrium* (Cestoda: Onchoproteocephalidea: Onchobothriidae) from *Dasyatis akajei* (Myliobatiformes: Dasyatidae) in the China Sea. *Zootaxa* 4169, 286–300.
- Zaragoza-Tapia, F., Pulido-Flores, G., Violante-González, J., Monks, S., 2019. Two new species of *Acanthobothrium* Blanchard, 1848 (Onchobothriidae) in *Narcine entemedor* Jordan & Starks, 1895 (Narcinidae) from Acapulco, Guerrero, Mexico. *ZooKeys* 852, 1–21.
- Zaragoza-Tapia, F., Pulido-Flores, G., Gardner, S.L., Monks, S., 2020a. Host relationships and geographic distribution of species of *Acanthobothrium* Blanchard, 1848 (Onchoproteocephalidea, Onchobothriidae) in elasmobranchs: a metadata analysis. *ZooKeys* 940, 1–49.
- Zaragoza-Tapia, F., Pulido-Flores, G., Monks, S., 2020b. Three new species of *Acanthobothrium* Blanchard, 1848 (Cestoda: Onchoproteocephalidea) in stingrays (Dasyatidae) from the Pacific coast in Mexico. *Zootaxa* 4766, 139–172.